

1 | **Revision 1**

2

3 | **Lightning-induced shock lamellae in quartz**

4

5 | Reto Gieré ^{a,*}, Wolfhard Wimmenauer ^b, Hiltrud Müller-Sigmund ^b, Richard Wirth ^c,
6 | Gregory R. Lumpkin ^d, and Katherine L. Smith ^e

7

8

9 | ^a Department of Earth and Environmental Science, University of Pennsylvania,

10 | Philadelphia, PA 19104-6316, USA.

11 | ^b Institut für Geo- und Umweltwissenschaften, Albert-Ludwigs-Universität 79104

12 | Freiburg, Germany.

13 | ^c GeoForschungsZentrum Potsdam, Department 4, Telegrafenberg, 14473 Potsdam,

14 | Germany.

15 | ^d Institute of Materials Engineering, ANSTO, Private Mail Bag 1, Menai, NSW 2234,

16 | Australia.

17 | ^e International Relations, ANSTO, P.O. Box 2001, Kirrawee DC, NSW 2232, Australia.

18

19

20

21 | * Corresponding author. Phone: (215) 898-6907.

22 | *E-mail address:* giere@sas.upenn.edu

23

24

ABSTRACT

25 Using transmission electron microscopy we show that planar deformation lamellae occur
26 within quartz in the substrate of a rock fulgurite, i.e., a lightning-derived glass. These
27 lamellae exist only in a narrow zone adjacent to the quartz/fulgurite boundary and are
28 comparable to planar deformation features (“shock lamellae”) caused by hypervelocity
29 impacts of extra-terrestrial objects. Our observations strongly suggest that the lamellae
30 described here have been formed as a result of the fulgurite-producing lightning strike.
31 This event must have generated a transient pressure pulse, whose magnitude, however, is
32 uncertain at this stage.

33

34 **Keywords:** shock lamellae, fulgurite, lightning, planar deformation features,
35 transmission electron microscopy

36

37

38

INTRODUCTION

39 On average, a total of nearly 1.4 billion lightning discharges occur annually around the
40 globe, equivalent to an average of 44 ± 5 lightning flashes per second, of which
41 approximately 10% are typically ground strikes (Christian et al., 2003). Cloud-to-ground
42 lightning strikes are highly energetic and very short events (millisecond range; see Rakov
43 and Uman, 2006; Uman et al., 1978) with peak lightning currents that are typically on the
44 order of tens of kA (MacGorman and Rust, 1998), but may exceed 200 kA (Rakov and
45 Uman, 2006). As the electrical resistance of air at ambient temperature is large, the air is
46 rapidly heated when such large currents flow through it (MacGorman and Rust, 1998),

47 leading to instantaneous peak air temperatures of 25,000-30,000 K (Rakov and Uman,
48 2006). Highly energetic lightning can dissipate a total of 1-10 GJ over the extensive
49 channel in a cloud, of which 1-10 MJ are estimated to be delivered to the strike point
50 (Borucki and Chameides, 1984; Rakov and Uman, 2006). This energy transfer may cause
51 rapid heating of the target material to temperatures above 2000 K (Essene and Fisher,
52 1986; Frenzel et al., 1989; Pasek and Block, 2009) as well as rapid physical and chemical
53 changes (Appel et al., 2006; Essene and Fisher, 1986; Frenzel et al., 1989; Pasek and
54 Block, 2009), and results in the formation of fulgurites, i.e., natural glasses produced by
55 fusion of rock, unconsolidated sediments, or soils through cloud-to-ground lightning
56 (Pasek et al., 2012). As the energy transfer is so fast, high-energy lightning flashes may
57 also cause high pressures (> 10 GPa?) when they strike the ground, possibly leading to
58 shock metamorphic effects in the target material (Collins et al., 2012; Frenzel et al., 1989;
59 Wimmenauer, 2003).

60 The aim of this study is to report evidence, collected using transmission electron
61 microscopy (TEM), for the presence of shock lamellae in a quartz crystal, which forms
62 the substrate of a rock fulgurite found at Les Pradals, France. In this brief paper, we will
63 not present the mineralogical and microstructural details of the actual fulgurite.

64

65

66

MATERIALS AND METHODS

67 Polished thin sections (~ 30 μm thick) of a hand specimen from Les Pradals, France
68 were first investigated with a petrographic microscope, using plane-polarized, cross-
69 polarized, and reflected light. Subsequently, one of the thin sections was coated with 20

70 nm of carbon and studied in back-scattered electron (BSE) mode with a CAMECA SX-
71 100 electron microprobe (EMP) equipped with five wavelength-dispersive crystal
72 spectrometers, which were used for quantitative chemical analysis of individual minerals
73 in the granite substrate and of the fulgurite matrix. The analytical conditions were as
74 follows: an acceleration voltage of 15 kV; a beam current of 10 nA, measured on a
75 Faraday cup; and a beam diameter of 3-8 μm . Synthetic and natural international
76 reference materials were used as standards. Due to the porous structure of the fulgurite
77 matrix, chlorine was analyzed to monitor the influence of the embedding epoxy, but its
78 contents usually lay below the detection limit. Counting time on peak positions was 8-10
79 s (to keep heating of the delicate glass structure as low as possible), and typically half of
80 that on the background positions on either side of the peaks. The raw data were corrected
81 using the PAP procedure (Pouchou and Pichoir, 1984).

82 Foils used for the TEM investigation were cut from one of the studied thin sections
83 using an FEI FIB200 focused ion beam (FIB) milling instrument (Wirth, 2004). The areas
84 to be cut were coated with a 1 μm thick platinum layer to reduce charging and cut using
85 30 kV gallium ions. The cuts were made perpendicular to the surface of the carbon-
86 coated thin section, yielding TEM-ready foils ($\sim 15 \times 10 \times 0.15 \mu\text{m}$), which were placed
87 onto a lacy-carbon copper grid.

88 The TEM investigations were carried out at 200 kV with a FEI Tecnai F20 X-Twin
89 instrument, equipped with a high-angle annular dark field detector and an energy-
90 dispersive X-ray spectrometer, which allowed for qualitative compositional analysis.

91

92

93

RESULTS AND DISCUSSION

94 **Field Observations**

95 At Les Pradals, Commune de Mons, Département Hérault (France) lightning struck a
96 coarse-grained granitic rock (grain size: 5-10 mm across) consisting of quartz, potassium
97 feldspar, albite, muscovite, and bluish tourmaline (schorl), as well as accessory Mn-rich
98 almandine garnet, apatite, and zircon. The studied fulgurite occurrence is one of several
99 similar finds, formed by lightning impact on granite and metamorphic rocks of the
100 region, and testifies to the extraordinary violence of such events.

101 The outcrop shown in Figure 1a has been blown apart along earlier fissures, scattering
102 meter-sized angular blocks in the dense brushwood vegetation surrounding it. The rock
103 body left in place shows blackish decorations on all prominent edges and fractures and
104 exhibits similar dark crusts on the adjoining surfaces (Fig. 1b, 1c). These crusts terminate
105 typically along the edges of quartz or feldspar fracture planes and may be reduced to
106 small droplets on exposed crystal faces (Fig. 1d). Documented lightning strikes have
107 produced similar blast characteristics and vitreous surface coatings on silicate rocks and
108 masonry in the Schwarzwald ("Black Forest", Germany), Vosges (France), and other
109 regions (Appel et al., 2006; Müller-Sigmund and Wimmenauer, 2002; Wimmenauer,
110 2003; Wimmenauer, 2006; Wimmenauer and Wilmanns, 2004; Gieré, unpublished
111 work). The continuous surface coatings of the Les Pradals fulgurite cover areas of several
112 square centimeters to square decimeters and exhibit a thickness of only a few tens of
113 micrometers. This appearance is distinct from typical rock fulgurites, which are melt
114 coats limited to small impact spots (Frenzel et al., 1989; Grapes and Müller-Sigmund,
115 2009; Pasek et al., 2012).

116

117 **Characterization by optical and scanning electron microscopy**

118 Observation with an optical microscope shows the blackish coating noted in the field
119 to be a thin, nearly opaque layer (Fig. 2a) of fairly constant thickness, only locally
120 exceeding 50 μm (Fig. 2b, 2c). The fulgurite layer consists of an optically isotropic
121 matrix, in which many small ($< 1 \mu\text{m}$ to several μm across) non-isotropic mineral
122 inclusions are embedded. The matrix also contains black, carbonaceous particles, which
123 cause the observed opacity.

124 Examination of polished sections by reflected light microscopy revealed that the
125 fulgurite layer is highly vesicular, a typical feature of fulgurites caused by vaporization of
126 rocks struck by lightning (Essene and Fisher, 1986; Frenzel et al., 1989; Frenzel and
127 Ottemann, 1978; Grapes and Müller-Sigmund, 2009; Martin Crespo et al., 2009). This
128 vesicular appearance is also observed in BSE images, which further reveal that the
129 fulgurite layer is heterogeneous, showing strong grey-scale contrast due to variations in
130 the mean atomic number of the phases present (Fig. 2b, 2c). Fractures cut parts of the
131 layer or, in some cases, the entire fulgurite layer (Fig. 2c). In some places the fulgurite
132 layer is separated from the granitic substrate by cracks, which are roughly parallel to the
133 substrate surface (Fig. 2b). These cracks were most probably caused by sample
134 preparation.

135

136 **Fulgurite composition**

137 The chemical composition of the fulgurite matrix was determined by spot analyses
138 using an EMP. As a result of the high porosity of the fulgurite layer (Fig. 2c), the

139 analytical totals of the EMP data are low, typically between 80 and 90 wt%. The glassy
140 fulgurite matrix contains on average 69 ± 6 wt% SiO_2 and is poor in total alkalis (Table
141 1), and thus may be classified as dacite according to the $\text{Na}_2\text{O}+\text{K}_2\text{O}$ vs. SiO_2
142 nomenclature of Middlemost (1994). The composition of the fulgurite matrix is relatively
143 homogeneous, and the concentrations of CaO, Na_2O , and K_2O are always low,
144 irrespective of the substrate mineral (quartz, albite, potassium feldspar or muscovite). The
145 elevated contents of P_2O_5 and SO_2 (Table 1) cannot be attributed to these substrate
146 minerals and thus, given the presence of lichen on many surfaces not covered by
147 fulgurite, may result from biogenic material present on the rock surface at the time of the
148 lightning strike. A relatively high phosphorus content, however, is not unusual for
149 fulgurites (Grapes and Müller-Sigmund, 2009; Martin Crespo et al., 2009; Pasek and
150 Block, 2009; Pasek et al., 2012). We were unable to determine the bulk carbon content of
151 the fulgurite layer at Les Pradals due to its extreme thinness. However, another fulgurite
152 we studied from the nearby locality of Bardou contains approximately 18 wt% elemental
153 carbon (determined with a LECO RC-412 multiphase carbon analyzer).

154

155 **Characterization by transmission electron microscopy**

156 The TEM investigation showed that the fulgurite matrix is entirely amorphous.
157 Embedded in this non-crystalline matrix, however, are various mineral grains and pores.
158 The pores are typically elongated and aligned in a direction that is parallel to the
159 boundary between substrate and fulgurite (Fig. 3a). In many areas of the fulgurite matrix,
160 the pores are aligned around the embedded crystals, resembling flow textures in volcanic

161 glass (Vernon, 2000). Minerals identified so far in the fulgurite glass include quartz,
162 hematite, magnetite, strontium-bearing barite, chlorite, and a 10-Å sheet silicate.

163 In a quartz grain located at the interface between the fulgurite layer and the substrate
164 (position #1 in Fig. 2b), we observed a set of distinct, sharp, remarkably straight, and
165 parallel lamellae (Fig. 3). These lamellae are comparable in appearance to the planar
166 deformation features (PDFs) observed by TEM in quartz from rocks that were subjected
167 to shock metamorphism as a result of a meteorite or experimental projectile impact at
168 pressures > 10 GPa (Ashworth and Schneider, 1985; French and Koeberl, 2010; Goltrant
169 et al., 1991; Langenhorst and Deutsch, 2012; Stöffler and Langenhorst, 1994). The
170 lamellae studied here are partially crystalline, as seen in dark-field TEM images (Fig. 3b).
171 Lamellae were observed only in a narrow zone (2.8 – 3.2 μm wide), which extends from
172 the fulgurite/substrate interface into the interior of quartz and terminates in a sharp
173 boundary with a lamella-free zone (left-hand side of Fig. 3c). We interpret this abrupt
174 termination as the boundary between compressed and uncompressed areas (i.e., the shock
175 front) and indicative of where the compressive force dropped below the threshold value
176 for quartz to record it in the form of lamellae.

177 The spacing between adjacent lamellae varies between 51 and 333 nm, with an
178 average of 152 ± 58 nm (28 measurements). Close inspection of Figure 3c reveals that
179 some of the lamellae show bifurcations, implying that not all the lamellae are strictly
180 parallel to each other. However, the planar nature of these lamellae and the absence of
181 dislocation arrays exclude the possibility that they might represent sub-grain boundaries.
182 The lamellae are oriented at an acute angle to the substrate/fulgurite interface. Further

183 away from the fulgurite/substrate boundary, in the interior of the substrate (position #2 in
184 Fig. 2b), the quartz does not display any PDFs.

185 Despite the high susceptibility of quartz to damage by the electron beam, we were able
186 to obtain a high-resolution TEM image of one lamella from the area shown in Figure 3a
187 using very short exposure time (0.2 s). This image (Fig. 4a) was used to create a fast-
188 Fourier-transformation image, which allowed us to index the resulting diffraction spots.
189 Our analysis revealed that the lamellae are oriented parallel to $(01\bar{1}0)$ of quartz (Fig. 4b),
190 which corresponds to one of the prism faces.

191

192

193 **IMPLICATIONS**

194 The orientation of the lamellae described here corresponds to the composition plane of
195 Dauphiné twins, which can be induced by applied pressure, by beta-alpha quartz
196 transition on cooling, and by intense dynamic stresses (e.g., meteorite impacts, seismic
197 rupture; see Wenk et al., 2011). The lamella orientation observed in our sample is
198 different from that reported for quartz affected by meteorite impacts or experimental
199 shock load, where the PDFs are most commonly parallel to the $\{0001\}$ basal planes or, at
200 high pressures, parallel to the $(10\bar{1}n)$ rhombohedral planes, where $n = 0$ (rare), 1, 2, 3, and
201 4 (Ferrière et al., 2009; Grieve et al., 1996; Stöffler and Langenhorst, 1994). Another
202 difference to observations of quartz impacted by a high-velocity solid projectile is that in
203 quartz from Les Pradals the lamellae are not visible optically in the narrow ($\sim 3 \mu\text{m}$)
204 deformation zone. However, previous optical studies on wider ($\sim 30 \mu\text{m}$) shock zones
205 within fulgurite substrates at other localities reported the occurrence of planar

206 deformation lamellae, albeit without TEM evidence (see photomicrographs in Frenzel et
207 al., 1989). In combination with the indirect evidence provided by neutron diffraction data
208 (Ende et al., 2012) and with theoretical considerations (Collins et al., 2012), our study
209 shows that lightning is indeed capable of producing shock lamellae in minerals.

210

211

ACKNOWLEDGMENTS

212 R.G. is grateful for the financial support from ANSTO and for access to the TEM facility
213 at GFZ Potsdam. We thank D. Rumble, E. Bruning, M.R. Dury and an anonymous
214 reviewer as well as the editors C. Hetherington and I. Swainson for their criticism and
215 very helpful comments on an earlier version of this manuscript.

216

217

218

REFERENCES CITED

- 219 Appel, P.W.U., Abrahamsen, N., and Rasmussen, T.M., 2006. Unusual features caused by
220 lightning impact in West Greenland. *Geological Magazine*, 143(5), 737-741.
- 221 Ashworth, J.R., and Schneider, H., 1985. Deformation and transformation in experimentally
222 shock-loaded quartz. *Physics and Chemistry of Minerals*, 11, 241-249.
- 223 Borucki, W.J., and Chameides, W.L., 1984. Lightning - estimates of the rates of energy
224 dissipation and nitrogen fixation. *Reviews of Geophysics and Space Physics*, 22, 363-
225 372.
- 226 Christian, H.J., Blakeslee, R. J., Boccippio, D. J., Boeck, W. L., Buechler, D. E., Driscoll, K. T.,
227 Goodman, S. J., Hall, J. M., Koshak, W. J., Mach, D. M. & Stewart, M. F., 2003. Global

- 228 frequency and distribution of lightning as observed from space by the Optical Transient
229 Detector. *Journal of Geophysical Research*, 108 (D1), ACL-1 – ACL-15.
- 230 Collins, G.S., Melosh, H.J., and Pasek, M.A., 2012. Can lightning strikes produce shocked
231 quartz? 43rd Lunar and Planetary Science Conference Abstract #1160.
- 232 Ende, M., Schorr, S., Kloess, G., Franz, A., and Tovar, M., 2012. Shocked quartz in Sahara
233 fulgurite. *European Journal of Mineralogy*, 24, 499-507.
- 234 Essene, E.J., and Fisher, D.C., 1986. Lightning strike fusion: extreme reduction and metal-silicate
235 liquid immiscibility. *Science*, 234, 189-193.
- 236 Ferrière, L., Morrow, J.R., Amgaa, T., and Koeberl, C., 2009. Systematic study of universal-stage
237 measurements of planar deformation features in shocked quartz: Implications for
238 statistical significance and representation of results. *Meteoritics & Planetary Science*,
239 44/6, 925-940.
- 240 French, B.M., and Koeberl, C., 2010. The convincing identification of terrestrial meteorite impact
241 structures: What works, what doesn't, and why. *Earth-Science Reviews*, 98, 123-170.
- 242 Frenzel, G., Irouschek-Zumthor, A., and Stähle, V., 1989. Stoßwellenmetamorphose,
243 Aufschmelzung und Verdampfung bei Fulguritbildung an exponierten Berggipfeln.
244 *Chemie der Erde*, 49, 265-286.
- 245 Frenzel, G., and Ottemann, J., 1978. Über Blitzgläser vom Katzenbuckel (Odenwald) und ihre
246 Ähnlichkeit mit Tektiten. *Neues Jahrbuch für Mineralogie – Monatshefte*, 439-446.
- 247 Goltrant, O., Cordier, P., and Doukhan, J.-C., 1991. Planar deformation features in shocked
248 quartz; a transmission electron microscopy investigation. *Earth and Planetary Science*
249 *Letters*, 106, 103-115.

- 250 Grapes, R., and Müller-Sigmund, H., 2009. Lightning-strike fusion of gabbro and formation of
251 magnetite-bearing fulgurite, Cornone di Blumone, Adamello, Western Alps, Italy.
252 Mineralogy & Petrology, 99, 67-74.
- 253 Grieve, R.A.F., Langenhorst, F., and Stöffler, D., 1996. Shock metamorphism in quartz in nature
254 and experiment: II. Significance in geoscience. Meteoritics and Planetary Science, 31, 6-
255 35.
- 256 Langenhorst, F., and Deutsch, A., 2012. Shock metamorphism of minerals. Elements, 8, 31-36.
- 257 MacGorman, D.R., and Rust, W.D., 1998. The Electrical Nature of Storms. Oxford University
258 Press.
- 259 Martin Crespo, T., Lozano Fernandez, R.P., and Gonzalez Laguna, R., 2009. The fulgurite of
260 Torre de Moncorvo (Portugal): description and analysis of the glass. European Journal of
261 Mineralogy, 21, 783-794.
- 262 Middlemost, E.A.K., 1994. Naming materials in the magma/igneous rock system. Earth-Science
263 Reviews, 37, 215-224.
- 264 Müller-Sigmund, H., and Wimmenauer, W., 2002. Fulgurite im Schwarzwald (BRD) und im
265 Massif Central (F). Berichte der Deutschen Mineralogischen Gesellschaft, 1, 115.
- 266 Pasek, M.A., and Block, K., 2009. Lightning-induced reduction of phosphorus oxidation state.
267 Nature Geoscience, 2, 553-556.
- 268 Pasek, M.A., Block, K., and Pasek, V., 2012. Fulgurite morphology: a classification scheme and
269 clues to formation. Contributions to Mineralogy and Petrology, 164, 477-492.
- 270 Pouchou, J.L., and Pichoir, F., 1984. Un nouveau modèle de calcul pour la microanalyse
271 quantitative par spectrométrie de rayons X. Partie I: Application à l'analyse d'échantillons
272 homogènes. Recherches Aérospatiales, 1984-3, 167-192.

- 273 Rakov, V.A., and Uman, M.A., 2006. Lightning: Physics and Effects. Cambridge University
274 Press, Cambridge.
- 275 Stöffler, D., and Langenhorst, F., 1994. Shock metamorphism of quartz in nature and experiment:
276 I. Basic observation and theory. *Meteoritics*, 29, 155-181.
- 277 Uman, M.A., Beasley, W. H., Tiller, J. A., Lin, Y., Krider, E. P., Weidmann, C. D., Krehbiel, P.
278 R., Brook, M., Few, A. A., Brohannon, J. L., Lennon, C. L., Poehler, H. A., Jafferis, W.,
279 Gulick, J. R. & Nicholson, J. R., 1978. An unusual lightning flash at Kennedy Space
280 Center. *Science*, 201, 9-16.
- 281 Vernon, R.H., 2000. Review of microstructural evidence of magmatic and solid-state flow.
282 *Electronic Geosciences*, 5, 1-23.
- 283 Wenk, H.-R., Janssen, C., Kenkmann, T., and Dresen, G., 2011. Mechanical twinning in quartz:
284 Shock experiments, impact, pseudotachylites and fault breccias. *Tectonophysics*, 510, 69-
285 79.
- 286 Wimmenauer, W., 2003. Wirkungen des Blitzes (Sprengung und Fulguritbildung) an Felsen im
287 Schwarzwald. *Berichte der Naturforschenden Gesellschaft zu Freiburg i. Br.*, 93, 1-32.
- 288 Wimmenauer, W., 2006. Vorkommen und Strukturen von Fulguriten im Schwarzwald. *Der*
289 *Aufschluss*, 57, 325-328.
- 290 Wimmenauer, W., and Wilmanns, O., 2004. Neue Funde von Blitzsprengung und Fulguritbildung
291 im Schwarzwald. *Berichte der Naturforschenden Gesellschaft zu Freiburg i. Br.*, 94, 1-22.
- 292 Wirth, R., 2004. Focused ion beam (FIB): a novel technology for advanced application of micro-
293 and nanoanalysis in geosciences and applied mineralogy. *European Journal of*
294 *Mineralogy*, 16, 863-876.
- 295
- 296

297

FIGURE CAPTIONS

298 **Figure 1.** Photographs taken at the studied fulgurite locality near Les Pradals, France. (a)
299 Photograph of the lightning-fractured outcrop. The surfaces facing the observer in upper
300 right are covered with black fulgurite. The block in the left foreground is approximately 2
301 meters high; (b) Detail of rock surface covered with the dark fulgurite coating. (c)
302 Fracture blackened by the lightning, which caused the black fulgurite coating. (d) Detail
303 of a feldspar surface, which is partially covered with dark, glassy fulgurite coatings in the
304 form of narrow decorations (left side of image) and small droplets (right side). The
305 pattern of black decorations seen in the upper left corner (photograph taken by P.
306 Rustemeyer) is reminiscent of a Lichtenberg figure.

307 **Figure 2.** Photomicrographs of the boundary between the fulgurite layer and its substrate.
308 (a) Thin section photograph, taken in plane-polarized light, showing the granitic rock
309 (lower left part of image) and the opaque to dark brown, thin fulgurite coating, which
310 traces the original rock surface. The granite is composed of clear quartz, turbid albite, and
311 bluish tourmaline (bottom left). Opaque areas within the rock are carbon-coating relics;
312 (b) BSE image of fulgurite rim (spongy texture) on quartz. It shows fractures crossing the
313 fulgurite layer, a crack separating it from the quartz substrate, and the two locations from
314 which focused ion beam foils were cut (#1, #2). Deformation bands were only seen in the
315 foil from position #1; (c) BSE image of foamy fulgurite layer mainly on quartz substrate.
316 Fulgurite contains inclusions of mineral fragments and micrometer-sized bright spheres
317 of variable composition, interpreted as captured fly ash particles. *Abbreviations:* Qtz =
318 quartz; Ab = albite.

319 **Figure 3.** Transmission electron microscope images of the granite/fulgurite interface. **(a)**
320 Bright-field image showing planar deformation lamellae in quartz (left), an iron-rich zone
321 at the interface within the fulgurite layer (dark, labeled as “Fe-rich”), and the amorphous
322 fulgurite with pores (bright lenticular features); **(b)** Dark-field image, obtained using
323 $(01\bar{1}0)$ of quartz, of the same area as that displayed in (a) showing the planar deformation
324 lamellae in quartz as set of bright, parallel bands crossing the image from upper right to
325 lower left; **(c)** Overview bright-field image showing undamaged quartz on the extreme
326 left, separated from lightning-damaged quartz by a sharp boundary, and the fulgurite
327 layer in the upper right. Dark shadow is an artifact due to the FIB sample preparation.
328 Image (a) shows detail from the upper right part of image (c), but it was taken first and
329 thus, does not show the electron beam damage to the lamellae seen in image (c).
330 *Abbreviations:* Qtz = quartz; F = fulgurite.

331 **Figure 4.** Transmission electron microscope image of a planar deformation lamella in
332 quartz. **(a)** High-resolution image showing a planar deformation lamella in quartz from
333 the area shown in Fig. 3a. The slightly brighter contrast of the deformation lamella shows
334 no lattice fringes thus indicating a non-crystalline state. The brighter contrast is due to
335 lower density of the non-crystalline material resulting in reduced mass absorption
336 contrast; **(b)** Fast-Fourier transformation image of the planar deformation lamella shown
337 in **(a)** displaying the diffraction spots with the respective Miller indices. Note the strong
338 diffuse scattering intensity from the non-crystalline part of the image.

339

340

341 **Table 1.** Bulk chemical composition
342 of the glassy fulgurite matrix (in
343 wt%), as determined by EMP
344 analysis.
345

Component	Average	σ_{n-1} ($n = 4$)
SiO ₂	69	6
TiO ₂	0.1	0.1
Al ₂ O ₃	9	2
FeO	2	2
MgO	0.8	0.4
CaO	1.3	0.5
Na ₂ O	0.2	0.1
K ₂ O	1.2	0.4
P ₂ O ₅	0.2	0.1
SO ₂	0.5	0.4
Total	84	

346
347

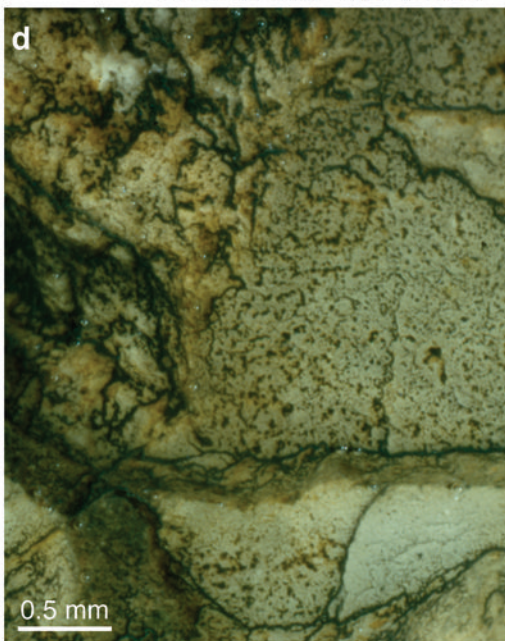
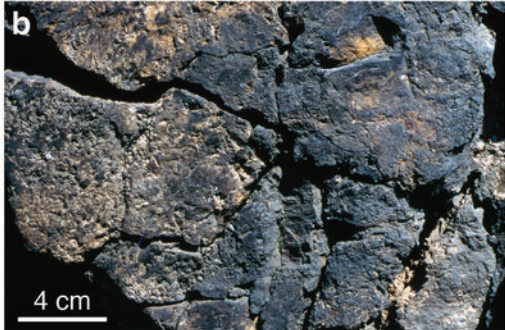


Fig. 1. Photographs taken at the studied fulgurite locality near Les Pradals, France.

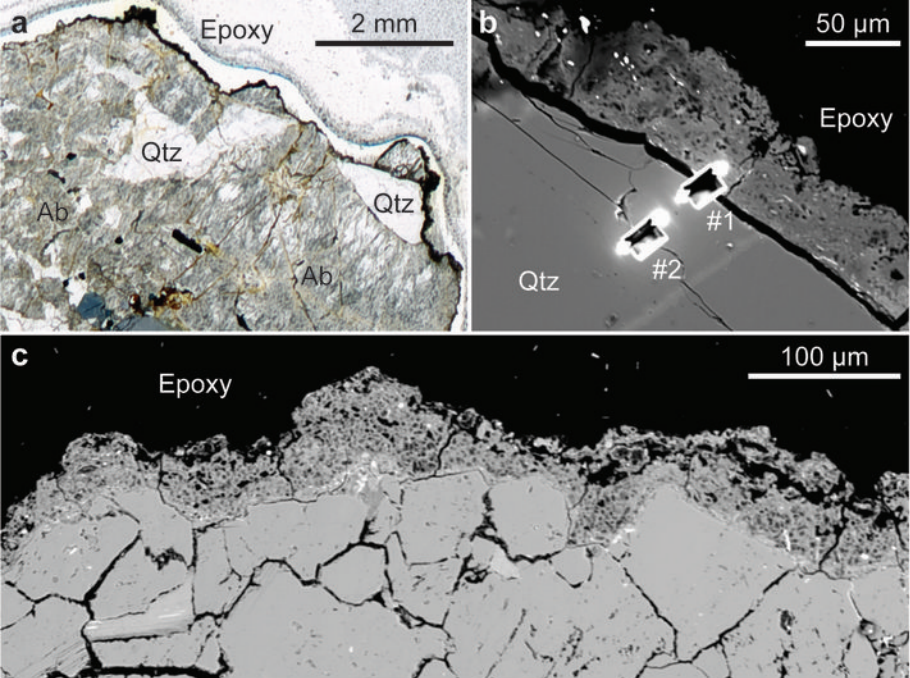


Fig. 2. Photomicrographs of the boundary between the fulgurite layer and its substrate.

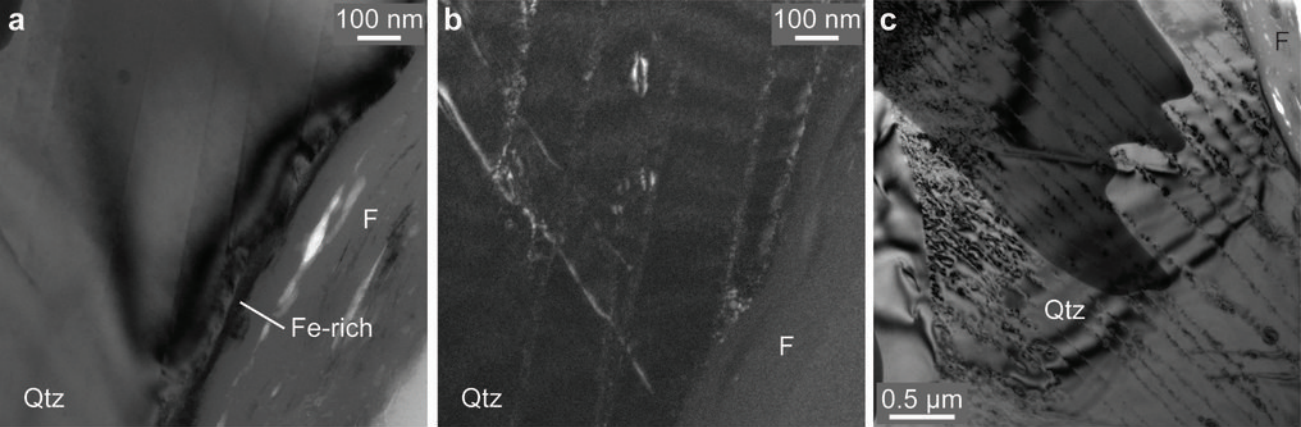


Fig. 3. Transmission electron microscope images of the granite/fulgurite interface.

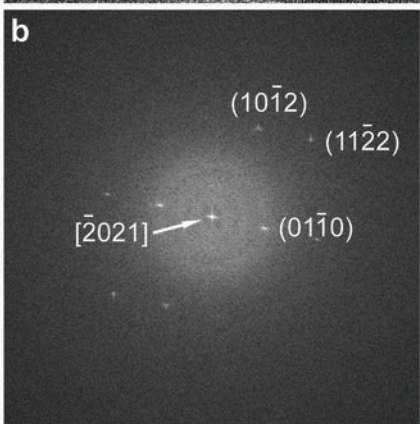
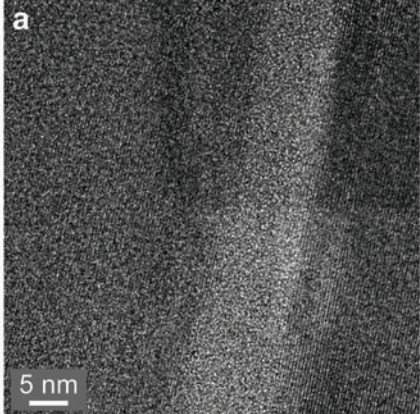


Fig. 4. Transmission electron microscope image of a planar deformation lamella in quartz.